(Online) ISSN 2744-1741
Defense and Security Studies *Original Research*
Vol. 5, No. 1, 2024, pp. 20-28
https://doi.org/10.37868/dss.v5.id204

Sub-6GHz hand pump shaped microstrip antenna for 5G communication

Adnan Ahmetović[1*], Şehabeddin Taha Imeci[2], Bilal Tütüncü[3]

[1] Electrical and Electronics Engineering, Faculty of Engineering and Natural Sciences, International University of Sarajevo, Bosnia and Herzegovina
[2] College of Engineering and Technology, American University of the Middle East, Kuwait
[3] Electrical and Electronics Engineering, Faculty of Engineering, Van Yüzüncü Yıl University, Van, Turkey

*Corresponding author E-mail: adnan.ahmetovic0@gmail.com

Received: Dec.10, 2023
Revised: Feb. 1, 2024.
Accepted: Mar. 3, 2024
Online: Mar. 8, 2024.

Abstract

The purpose of this paper is to explore the presented design of a hand-pump shaped microstrip antenna pfor sub-6GHz 5G communication. This paper will first provide a brief overview of the antenna design and its capabilities. Meaning, overall impressive dimensions of 25.25 mm x 20.75 mm x 1.55 mm, with S11 being -16.82 dB at operating frequency of 5.16 GHz. Next, the paper will discuss the design of the antenna and how it can be optimized with sub 6 GHz operating frequency, along with requirements. To reach required specifications, inc. E-$\theta \geq 5$ GHz $\geq$ E-φ; S11 $\leq$-10, various geometrical parameters, among others, have been tested, resulting in two slots being added (slot a and slot b), in combination with various slits. Finally, antenna is produced, and laboratory measurements are carried out for the validation of results. Further discussing potential benefits and drawbacks of using this antenna design for 5G applications.

Keywords: *hand-pump antenna, 5G, antenna analysis, sonnet software*

1. Introduction

5G networks operate in a higher frequency range than previous generations, allowing for faster speeds and more capacity. 5G signals are able to travel further and penetrate buildings better than previous generations, making it ideal for coverage in dense urban areas. 5G technology is also more energy efficient than earlier generations, meaning that service providers can deploy more 5G base stations without increasing power consumption. In terms of frequencies used, the 3.4 GHz-3.8 GHz band is at the forefront of the sub-6 GHz spectrum. Many countries see this band as a pioneer in realizing 5G technologies such as massive MIMO arrays and antennas [1-3]. In recent literature, there has been significant interest increase towards microstrip antennas, inc. single element antennas, MIMO antennas and arrays, for 5G application [4]. This paper is focused towards single element hand-pump shape microstrip patch antenna, using fr4 dielectric, which is known to have return loss is much lower compared to the other dielectric materials typically being used [5]. Based on the researches, we can see that both square and rectangular shaped microstrip patch antenna offers satisfactory value of return loss (S11), that can be reduced by proper selection of material and shape of the antenna [6, 7]. Antenna's shape fine design usually includes various slits and slots, which alter antenna parameters, by change of current distribution, along with use of different thicknesses [8, 9].

Based on the findings, we can conclude that using a substrate material with a greater dielectric constant degrades antenna performance while reducing antenna size. With increase of substrate thickness, the

resonance frequency results in decrease, in contrast to the bandwidth, which increases [10-11]. Paper [12] even suggests use of U Slotted Patch, along Air substrate, for better performance in terms of Gain. However, focus of this paper will achievement of desired parameters, which includes specifical vertical and horizontal polarization required values (- E-$\theta \geq$ 5 GHz $\geq$ E-φ), along with return loss (S11 $\leq$-10). Most of the wireless networks such as 5G require multiband MIMO-supported Base Station Antennas and achieve this with use of multiple ports, supporting wider range of frequencies, leading to multiple arrays within one compact antenna enclosure [13-15]. Paper [16] suggests employment of a single layer cross bow-tie dual-band tunable HIS (high-impedance surface) antenna designed for UHF band.

There is also the potential use of a waveguide simulator to characterize approximately the performance of the proposed metamaterial structure [17]. Patch array smart antennas can be used to arrange radiation patterns that cannot be achieved with a single patch element [18]. However, these structures of antennas require larger space, some have poor radiation efficiency and narrower bandwidth. Therefore, the focus of this paper, along others (S11, E-θ, E-φ) will be achievement of wider bandwidth, smaller size, and high gain performance at LTE 42/43 (3.4 GHz–3.8 GHz) band for 5G communication. This single band antenna is designed and analyzed in sonnet software [19], but also experimentally made. In addition, there is a lack of literature describing geometrical optimization of similar antennas. References [20] and [21] investigate the effect of the gap between radiating patches, but they do not take this into account to optimize the dimension parameters of a single-band antenna.

2. Method

Figure 1. represents Schematic Diagram of the Microstrip Patch Antenna, along with antenna dimensions. The design was created by joining together two rectangular shaped pieces. Antenna has dimensions of 25.25 mm x 20.75 mm x 1.55 mm and it is fed up via port in the bottom right. This configuration provided the best current distribution results. Design was created and simulated in Sonnet software, later on produced and experimentally tested. Initial design didn't satisfy required specifications, in terms of reflection loss (S11), so slits on the bottom right part were added, they improved S11 drastically, but still the E-θ was not sufficient, showing value much greater than -5 dB. To improve current distribution, along E-θ, a large slot in the middle was added, which resulted in value closer to the required -5 dB, but not yet sufficient. Furthermore, design was greatly improved, by detailed parametric analysis, resulting in two slots on the right, with one large slit in the middle, which, along dimension tweaking, provided sufficient results. More discussion along antenna dimensions can be seen in the Parametric Analysis part.

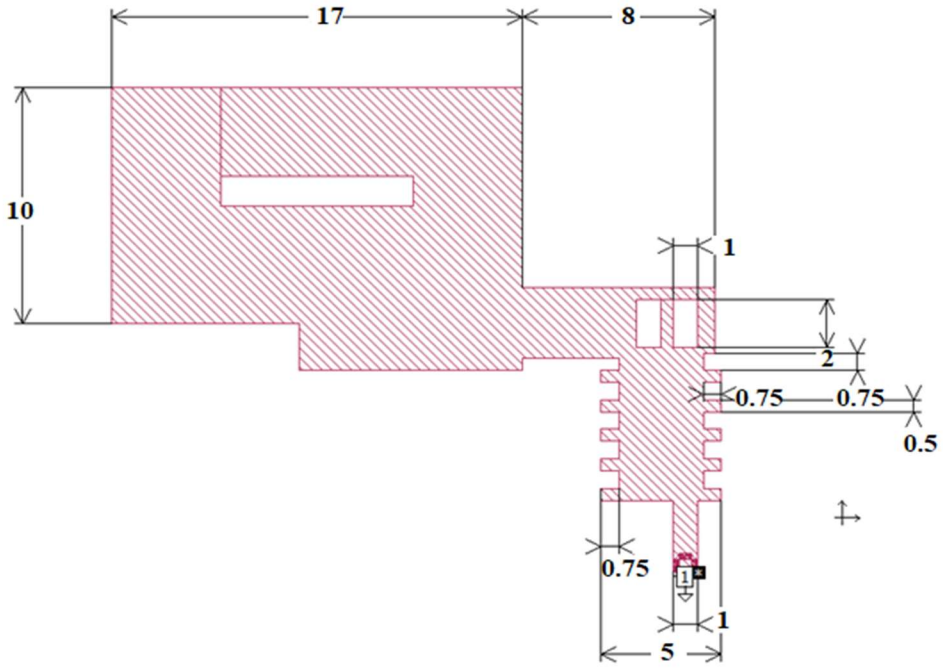

Figure 1. Schematic diagram of the microstrip patch antenna

Figure 2. represents 3D view of the antenna. It is noted that dielectric substrate material being used is FR4, with thickness of 1.55 mm. Already mentioned antenna feeding line, width of 1mm is drilled, so that port could be attached. For simulation purposes, box size was selected to be 10x larger than antennas dimensions, resulting in size of 225 mm x 255 mm. In this means cell size was 0.25 mm x 0.25 mm, which was minimum, limited by universities R&D equipment, preventing any circular elements in antenna's design, since they required smaller cell size to be properly design and simulated.

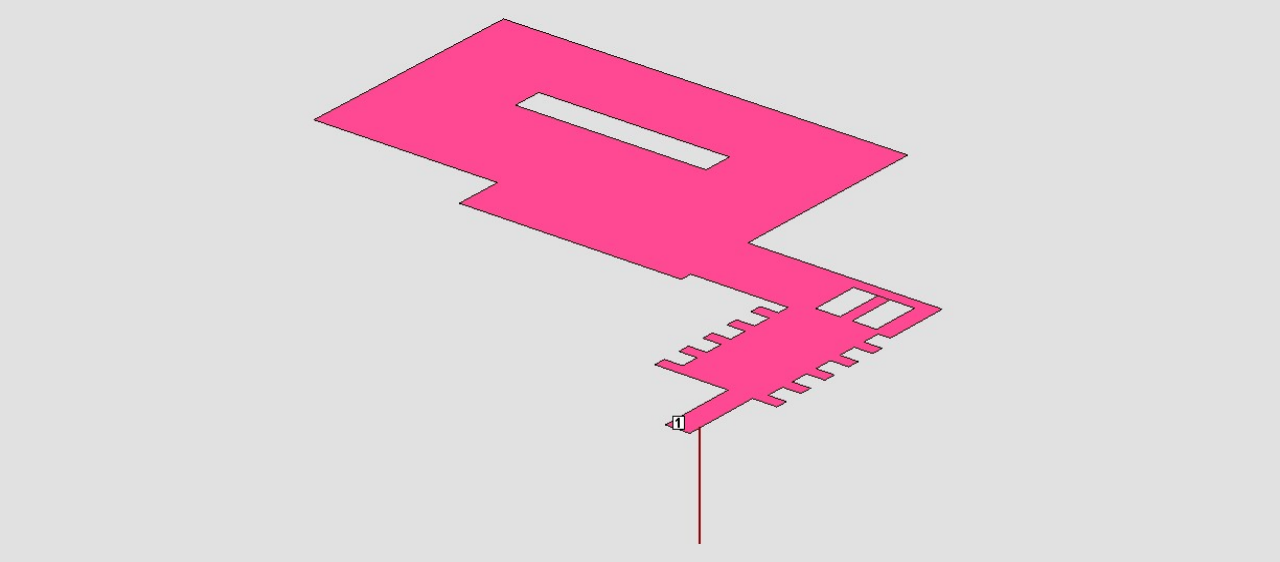

Figure 2. 3D view of the microstrip patch antenna

3. Results

Data shown below represents Parametric Analysis of proposed design. A parametric analysis was carried out by varying the dimensions of length and width of various antenna parts, as well as dielectric thickness and erel value. Analysis consists of 7 tables, where the first 3 tables represent size variations, Table 4 being Erel Value (ε_r in tables), Table 5 dielectric thickness and Table 6 and Table 7 are combination of previously done variations, with goal of choosing best value for every parameter.

Table 1. represents size variation of a Slot (a) (smaller slot on the right antenna side). It is noted that narrower slot design will result in S11 value fluctuation, with tendency to lower down, no matter the length. Value of 3 mm x 0.75 mm provided E-φ increase, but significantly decreases S11 value, therefore dimension of 2 mm x 1 mm is chosen.

Table 1. Size of the slot (a)

Dimension / mm	S11/ dB	Frequency / GHz	E-φ / dB	E-θ / dB
2 x 0.5	-13.71	5.26	5.362	-5.033
2 x 0.75	-13.85	5.26	5.372	-5.035
2.25 x 0.7	-13.63	5.26	5.382	-5.037
3 x 0.75	-12.81	5.24	5.414	-5.034
2 x 1	-13.90	5.26	5.384	-5.040

In Table 2., various dimensions have been proposed for Slot (b) (larger slot on the center part of the antenna), and it is noted that the length of the slot and S11 parameter are directly proportional, resulting in significant S11 value increase with length increase. Although S11 value has greatly increased, this option was not suitable, because E-θ value fell down below required (-5 dB), therefore, bolded dimensions were implemented.

Table 2. Size of the slot (b)

Slot-(b) Size/mm	S11/dB	Frequency/GHz	E-φ/dB	E-θ/dB
1.25 x 8	-13.70	5.26	5.343	-5.040
1.5 x 8	-15.24	5.22	5.379	-4.956
1.5 x 8.5	-20.36	5.12	5.262	-4.859
2.5 x 8.5	-18.14	4.98	5.145	-4.705
2 x 8.5	-18.45	5.06	5.389	-4.651

Table 3 represents results of various Slit dimensions (side rectangle on the bottom right of the antenna). Although some dimensions provided better E-φ and E-θ values, dimensions of 0.75 mm x 0.5 mm resulted in great S11 increase, hence it was more suitable. Less than 0.5 mm almost always resulted in E-φ decreas, in this case S11, also decreased.

Table 3. Size of the slits

Slits Size/mm	S11/dB	Frequency /GHz	E-φ/dB	E-θ /dB
1 x 0.5	-13.90	5.26	5.384	-5.040
1.25 x 0.5	-11.89	5.26	5.410	-5.026
1.5 x 0.5	-10.12	5.26	5.422	-5.093
0.75 x 0.5	-15.56	5.26	5.344	-5.026
0.75 x 0.25	-14.92	5.26	5.290	-5.026

Table 4. represents experimentation with Erel Value, it is noted that Erel Value of 4.6, although lowering the operating frequency of the antenna, increases both E-φ and E-θ, as well as S11, to -16.92 dB. Erel being lower than 4.4 results in E-θ decreasing below the required value of -5 dB.

Table 4. Erel value

ε_r	S11/dB	Frequency/GHz	E-φ/dB	E-θ/dB
4.4	-15.56	5.26	5.344	-5.026
4.5	-15.04	5.2	5.263	-5.121
4.6	-16.82	5.16	5.350	-5.147
4.3	-15.17	5.32	5.401	-4.931
4.2	-14.57	5.38	5.440	-4.844

Table 5. represents Dielectric Thickness fluctuation, while sticking to design default Erel Value of 4.2, note that any value less than 1.70 of diel. Thickness results in S11 above -15 dB, but any value lower than 1.55, reduces E-θ to less than -5 dB. With this, we can neglect the benefits of increased E-φ and S11 and stick to the value of 1.55.

Table 5. Dielectric thickness with erel value- (4.2)

Dielectric Thickness (ε_r- 4.2)	S11/dB	Frequency/GHz	E-φ/dB	E-θ/dB
1.55	-15.56	5.26	5.344	-5.026
1.6	-13.87	5.38	5.415	-4.765
1.65	-13.31	5.38	5.393	-4.683
1.52	-15.02	5.38	5.456	-4.890
1.45	-15.99	5.38	5.499	-4.988

In Table 6., we can see that now with Erel being value of 4.6, E-θ satisfies the requirements in every case, this provided ability to start experimenting with Dielectric Thickness more freely than before, hence value of dielectric thickness greater than 1.55 is not necessary, since it has negative result on S11, E-φ and E-θ. There is no need to lower down Diel. Thickness value, less than 1.55, since it satisfied the requirements, thicker dielectric layer can result in a more stable antenna design, while additionally increasing the power handling capability of the antenna.

Table 6. Dielectric thickness with erel value- (4.6)

Dielectric Thickness (ε_r- 4.6)	S11/dB	Frequency/GHz	E-φ/dB	E-θ/dB
1.55	-16.82	5.16	5.350 dB	-5.147 dB
1.6	-15.96	5.16	5.327 dB	-5.076 dB
1.65	-12.43	5.14	5.117 dB	-5.106 dB
1.52	-17.26	5.16	5.365 dB	-5.188 dB
1.45	-17.95	5.16	5.407 dB	-5.276 dB

Hence the above, Table 7 is representation of all the combined values, examining the S11 and radiation efficiency of the proposed antenna due to the optimized size parameters based on simulated results to achieve optimum values.

Table 7. Final parameters with chosen values.

Parameter	Value	S11	Frequency	E-φ	E-θ
Dielectric Thickness	1.55 mm	-16.71 dB	(5.16 GHz)	5.333 dB	-5.180 dB
ε_r	4.6				
Slot (a)	2 mm x 1 mm				
Slot (b)	1.25mm x 8mm				
Slit	0.75mm x 0.5mm				

4. Discussion

S-parameters are shown below (Figure 3.), specifically S11, representing reflection loss of the antenna. Already mentioned goal was to achieve S11 value of ≤ -10 dB, by this means S11 provided -16.71 dB, as seen below. This implies an operational frequency of 5.16 GHz, with an operational bandwidth of exactly 60 MHz. Furthermore, performance was studied with the help of antenna gain, current distribution, radiation pattern and radiation efficiency, specifical component shown in Figure 4 and Figure 5.

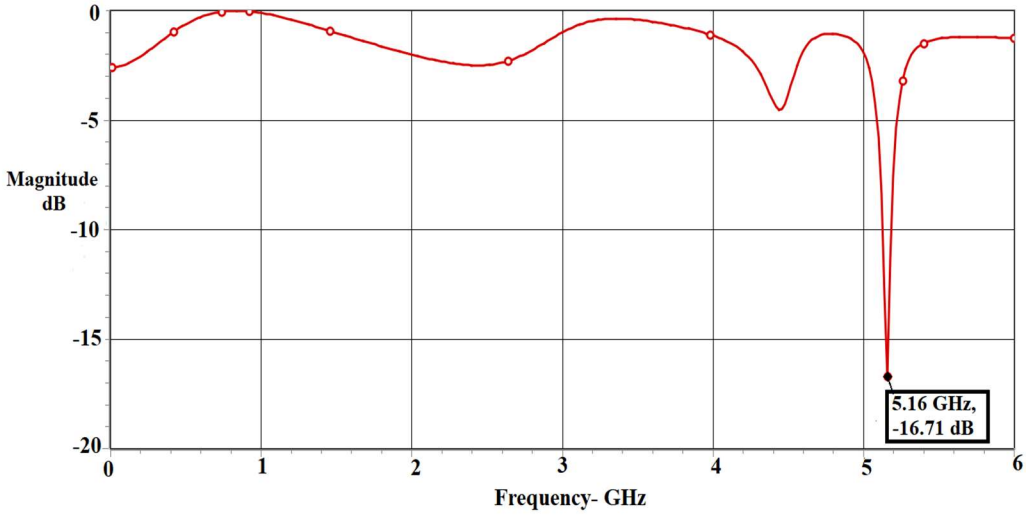

Figure 3. S-parameters of the microstrip patch antenna

Vertical polarization component (E-θ) is presented in Figure 4. Below, showing that E-θ is equal to -5.18 dB, at its peak point (50°), in operational frequency (5.16 GHz). This graph was the main point of concern, at particular the moment, since reaching desired values required numerus geometrical changes in antennas design.

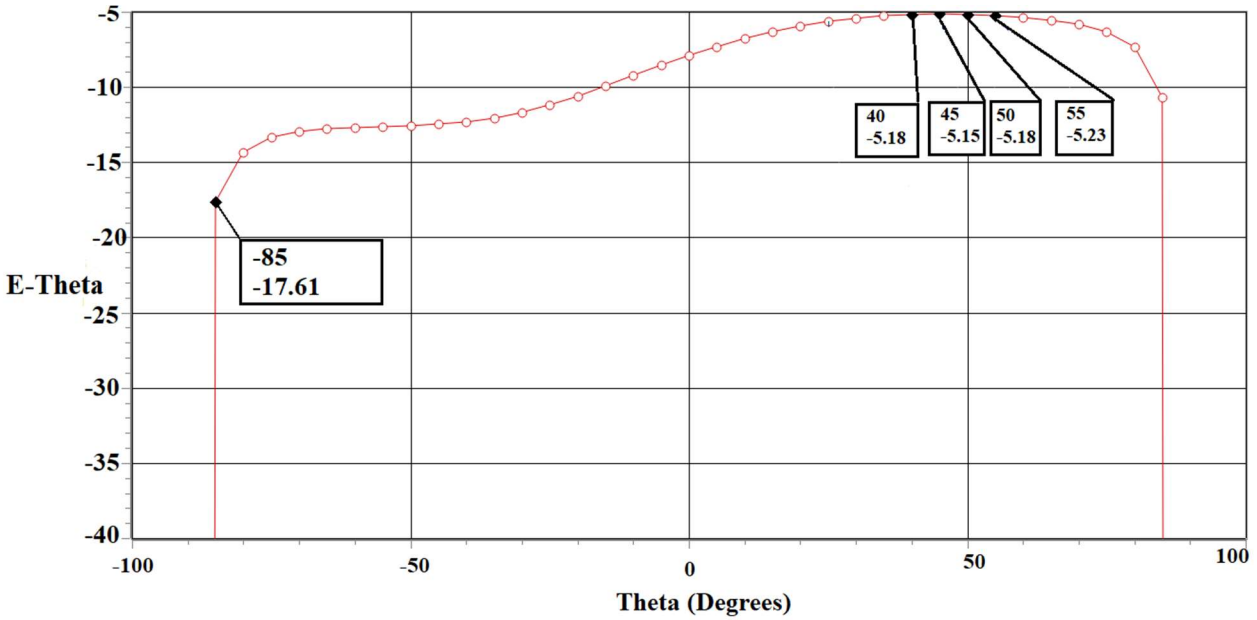

Figure 4. E-θ of the microstrip patch antenna

Horizontal polarization component (E-φ) is presented in Figure 5. It implies that E-φ reaches 5.333 dB, peak 5°. The presented simulation was done at frequency of 5.16 GHz. Moreover, in Figure 6. presenting Far Field with polar view including all curves together, it is noted that radiation pattern satisfied all the requirements.

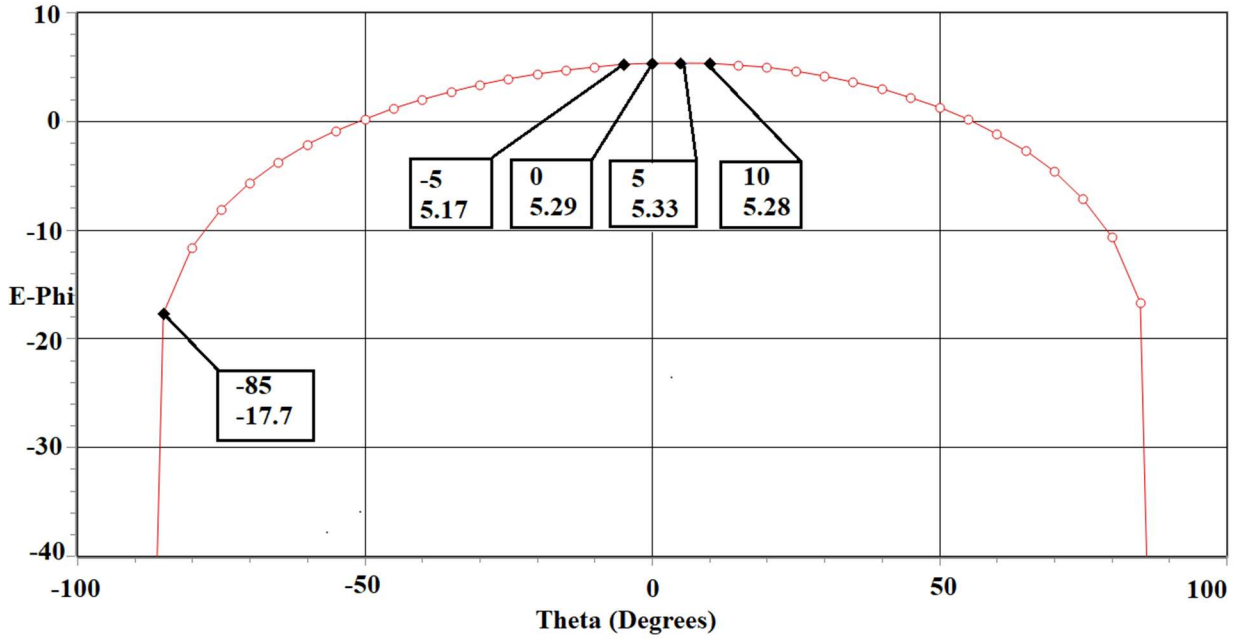

Figure 5. E-φ of the microstrip patch antenna

Presented Figure 6. considers all radiation pattern curves together in polar view, together with E-Total represented in yellow color. Red colored curve represents horizontal axis (E-φ), while vertical axis (E-θ) is represented in blue color. From the figure, the radiation pattern curves are close to symmetrical. Additionally, the maximum radiation intensity is located at the Theta=5°, showing 5.56 dB E-Total.

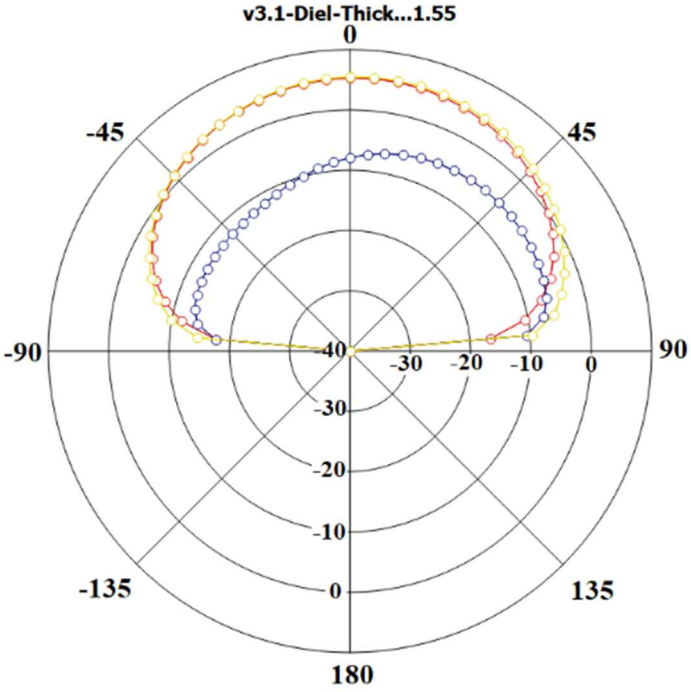

Figure 6. Radiation pattern of microstrip antenna

Figure 7. is showing circular E-Total polarization in 3D view, considering power gain with included reflection. Magnitude Scale is shown on the left. It can be seen that the polarization is quite good, with reflection well within the acceptable range, since values remand remarkably close to original.

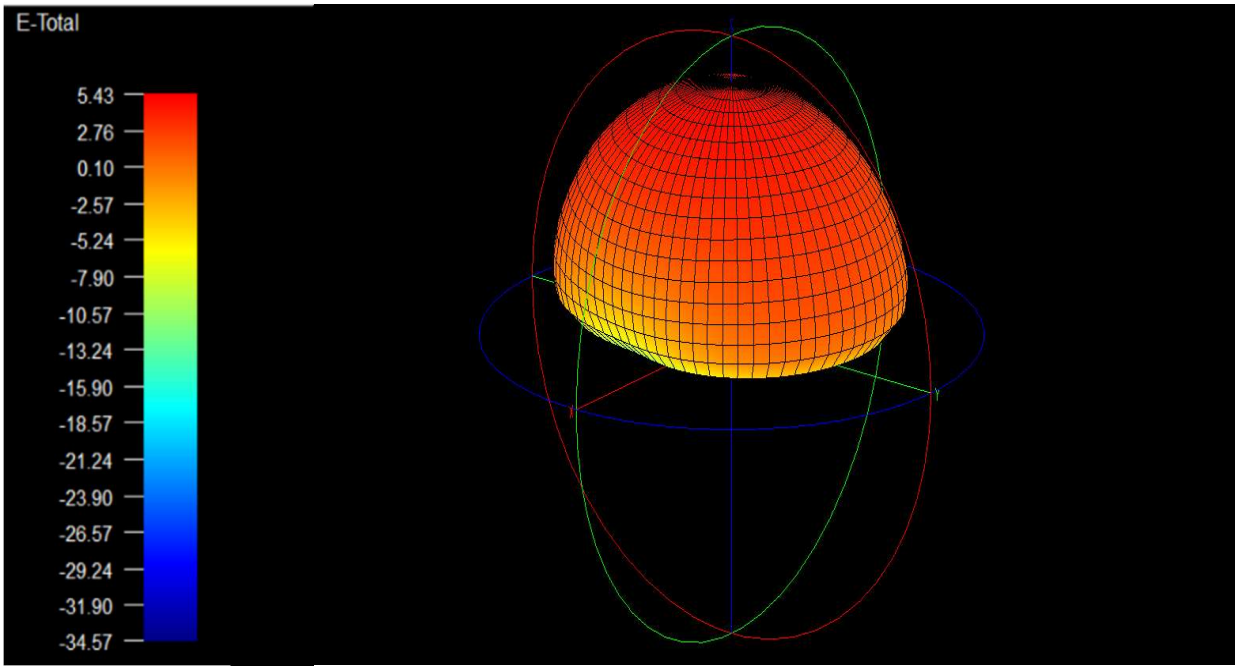

Figure 7. E-Total 3D view of microstrip patch antenna

Figure 8. represents current distribution diagram of presented antenna design, at 5.16 GHz. It is noted that current has tendency to flow from edges of the antenna to middle parts. This was the exact reason for adding large slot in the middle part. Graph proves that mentioned slot, increased current desnsity in area to values greater than 10 A/m. It can be seen that feeding line also, along with bottom right part plays particular role in current distribution, since changes in mentioned area, had lowered the magnitude in right part for consequence. By understanding the current distribution, the antenna design can be further improved to achieve better performance.

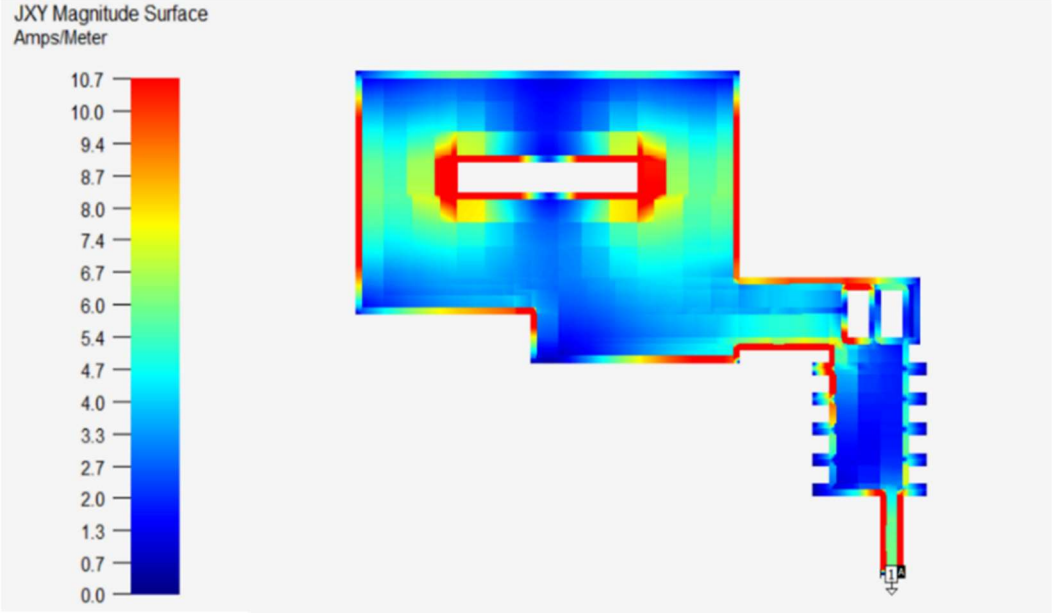

Figure 8. Current distribution of the microstrip patch antenna

In conclusion the proposed microstrip patch antenna shown in the paper, provides reflection loss of S11=-16.71 dB, E-φ of 5.333 dB and E-θ of -5.18 dB. This provides more than sufficient values for the sub 6GHz range. The design and geometrical optimization resulted in operational frequency of 5.16 GHz, with incredible dimensions, especially considering other single element-single port designs. Simulation was obtained using ABS sweeps, 0 GHz to 6 GHz, respectively. Furthermore, the proposed antenna design could be considered as a choice for 5G applications due to its high current density capability and small size. The slot in the middle part of the antenna plays the key role in increasing the current density, while the feeding line and the bottom right part also contribute to the current distribution. On the other hand, future geometrical improvements could be made with usage of optimization algorithms.

Funding information

This research received no specific grant from any funding agency in the public, commercial, or not-for-profit sectors.

Declaration of competing interest

The authors declare that they have no known competing financial interests or personal relationships that could have appeared to influence the work reported in this paper.

References

[1] N. Kaur, S. Sharma, and J. Kaur, "Performance comparison of evolutionary algorithms in the design of a hand-pump shape microstrip antenna for 5G applications", *Elektron. ir elektrotech.*, vol. 25, no. 5, pp. 31-36, 2019.

[2] N. Shoaib, S. Shoaib, R. Y. Khattak, I. Shoaib, X. Chen, and A. Perwaiz, "MIMO Antennas for Smart 5G Devices", *IEEE Access*, vol. 6, pp. 77014-77021, 2018.

[3] B. Tütüncü, "Microstrip Antenna for 5G Communication: Design and Performance Analysis", in *2020 International Congress on Human-Computer Interaction, Optimization and Robotic Applications (HORA)*, 2020.

[4] M. Pant and L. Malviya, "Design, developments, and applications of 5G antennas: a review", *Int. J. Microw. Wirel. Technol.*, pp. 1-27, 2022.

[5] M. Rastogi, "Design and analysis of microstrip patch antenna for different applications", *Int. J. Sci. Res. (Raipur)*, vol. 6, no. 12, pp. 421-424, 2017.

[6] S. Sharma, P. Kumar, R. Saraswat, and J. Jangir, "Performance analysis of square shaped microstrip patch antenna for S band application", *Int. J. Mod. Trends Eng. Res.*, vol. 3, no. 10, pp. 123-127, 2016.

[7] D. Vidhya, "Design and analysis of rectangular microstrip patch antenna", *Int. j. psychosoc. rehabil.*, vol. 24, no. 4, pp. 3723-3729, 2020.

[8] A. Akiyama, T. Yamamoto, M. Ando, and N. Goto, "Numerical optimisation of slot parameters for a concentric array radial line slot antenna", *IEE Proc. - Microw. Antennas Propag.*, vol. 145, no. 2, pp. 141, 1998.

[9] B. Tütüncü, H. Torpi, and Ş. T. İmeci, "Directivity improvement of microstrip antenna by inverse refraction metamaterial", *J. Eng. Res.*, vol. 7, no. 4, 2019.

[10] B. Tütüncü and M. Kösem, "Substrate analysis on the design of wide-band antenna for sub-6 GHz 5G communication", *Wirel. Pers. Commun.*, vol. 125, no. 2, pp. 1523-1535, 2022.

[11] D. C. and J. C. da S. Lacav, "Design of low-cost probe-fed microstrip antennas", in *Microstrip Antennas*, N. Nasimuddin, Ed. London, England: InTech, 2011.

[12] S. Rafi, "Gain enhancement of microstrip patch antenna by using novel air substrate with U-slotted patch," *Rev. Gest. Inov. Tecnol.*, vol. 11, no. 4, pp. 1017-1029, 2021.

[13] M. Farasat, D. N. Thalakotuna, Z. Hu, and Y. Yang, "A review on 5G sub-6 GHz base station antenna design challenges", *Electronics (Basel)*, vol. 10, no. 16, pp. 2000, 2021.

[14] N. Hussain, W. A. Awan, W. Ali, S. I. Naqvi, A. Zaidi, and T. T. Le, "Compact wideband patch antenna and its MIMO configuration for 28 GHz applications", *Int. J. Electron. Commun.*, vol. 132, no. 153612, pp. 153612, 2021.

[15] M. Ko, H. Lee, and J. Choi, "Planar LTE/sub-6 GHz 5G MIMO antenna integrated with mmWave 5G beamforming phased array antennas for V2X applications," *IET Microw. Antennas Propag.*, vol. 14, no. 11, pp. 1283–1295, 2020.

[16] H.-J. Lee, K. L. Ford, and R. J. Langley, "Independently tunable low-profile dual-band high-impedance surface antenna system for applications in UHF band", *IEEE Trans. Antennas Propag.*, vol. 60, no. 9, pp. 4092-4101, 2012.

[17] C. Mias and J. H. Yap, "A varactor-tunable high impedance surface with a resistive-lumped-element biasing grid", *IEEE Trans. Antennas Propag.*, vol. 55, no. 7, pp. 1955-1962, 2007.

[18] J. Mondal, S. Kumar Ray, M. S. Alam, and M. M. Rahman, "Design smart antenna by microstrip patch antenna array", *IACSIT int. j. eng. technol.*, vol. 3, no. 6, pp. 675-683, 2011.

[19] *Sonnet Software, version 18.52, www.sonnetsoftware.com, 2014*.

[20] G. Ram, D. Mandal, R. Kar, and S. P. Ghoshal, "Opposition-based BAT algorithm for optimal design of circular and concentric circular arrays with improved far-field radiation characteristics: Optimal Design of Circular and Concentric Circular", *Int. J. Numer. Model.*, vol. 30, no. 3-4, pp. e2087, 2017.

[21] D. W. Boeringer and D. H. Werner, "Particle swarm optimization versus genetic algorithms for phased array synthesis", *IEEE Trans. Antennas Propag.*, vol. 52, no. 3, pp. 771-779, 2004.